



# Determination of position-specific carbon isotope ratios of propane from natural gas

Yun Li<sup>a</sup>, Lin Zhang<sup>a,b</sup>, Yongqiang Xiong<sup>a,\*</sup>, Shutao Gao<sup>a</sup>, Zhiqiang Yu<sup>a</sup>, Ping'an Peng<sup>a</sup>

<sup>a</sup> State Key Laboratory of Organic Geochemistry (SKLOG), Guangzhou Institute of Geochemistry, Chinese Academy of Sciences, 511 Kehua Street, Wushan, Tianhe District, Guangzhou, Guangdong 510640, China

<sup>b</sup> University of Chinese Academy of Sciences, Beijing 100049, China

## ARTICLE INFO

### Article history:

Received 2 September 2017

Received in revised form 6 February 2018

Accepted 11 February 2018

Available online 12 February 2018

### Keywords:

Propane

Position-specific isotope analysis

Pyrolysis

Natural gas

## ABSTRACT

On-line gas chromatography–pyrolysis coupled to gas chromatography–isotope ratio mass spectrometry was used here for the position-specific isotope analysis (PSIA) of propane. First, based on the conversion rate of propane and its products, 800–840 °C was considered optimal for propane pyrolysis. The major pyrolytic fragments of propane included CH<sub>4</sub>, C<sub>2</sub>H<sub>4</sub>, C<sub>3</sub>H<sub>6</sub>, and C<sub>2</sub>H<sub>6</sub>. Subsequent isotope labeling experiments showed that CH<sub>4</sub> and C<sub>2</sub>H<sub>6</sub> were derived entirely from the terminal carbons, whereas C<sub>2</sub>H<sub>4</sub> and C<sub>3</sub>H<sub>6</sub> were derived from both terminal and central positions of propane. Therefore, the <sup>13</sup>C enrichment factor associated with the major reactions during the pyrolysis process and position-specific  $\delta^{13}\text{C}$  values of propane can be estimated from the amount and  $\delta^{13}\text{C}$  values of the pyrolytic fragments using isotope mass balance. The obtained enrichment factors depended on the pyrolysis temperature, which can be used to calculate position-specific  $\delta^{13}\text{C}$  values for propane measured with this system. The results suggest that a relatively accurate site-preference value for propane can be obtained by this method. Therefore, the combination of compound-specific isotope analysis and PSIA of propane will be a powerful tool to discriminate the different origins of gases.

© 2018 Elsevier Ltd. All rights reserved.

## 1. Introduction

Since the first coupling of commercial gas chromatography (GC) with a combustion furnace and isotope-ratio mass spectrometry (IRMS) was reported in 1990, compound-specific isotope analysis (CSIA) has become a powerful tool in many research fields (Hayes et al., 1990). However, the  $\delta^{13}\text{C}$  values measured by GC–IRMS represent an average distribution of carbon isotopes in a molecule, because all the measured compounds must combust to CO<sub>2</sub> before being transferred to the IRMS system. After Abelson and Hoering (1961) reported the enrichment of <sup>13</sup>C in the carboxyl positions in amino acids relative to other positions, various related investigations have demonstrated heterogeneous intramolecular isotopic distributions. Position-specific isotope analysis (PSIA), also called intramolecular or site-specific isotope analysis, can provide new insights into molecular origins, including formation pathways, by probing the isotope distributions of different positions within a molecule (Corso and Brenna, 1997).

Natural gases can be produced from kerogen, bitumen, or petroleum at different thermal maturity levels, and CSIA has been

widely used to identify their sources and determine their thermal maturity (Galimov, 1988; James, 1983, 1990; Rooney et al., 1995; Schoell, 1983, 1988). However, various factors affect the isotopic composition of natural gas, including its source, formation mechanism, migration, and biodegradation. The preferential breakage of <sup>12</sup>C–<sup>12</sup>C bonds during organic matter maturation results in <sup>13</sup>C-enrichment of the residual precursors and <sup>13</sup>C-depletion of the newly formed products. As maturation (and thus <sup>12</sup>C–<sup>12</sup>C bond breakage) progresses, the resulting <sup>13</sup>C-enrichment of the residual precursors will lead to any of the later-generated products being enriched in <sup>13</sup>C at the terminal carbon position relative to products formed earlier. During equilibrium fractionation, position-specific isotope enrichment results from homogeneous isotopic fractionation, which is independent of the isotope composition of the precursor material, but solely depends on the maturity of the source (Wang et al., 2004). However, during kinetic processes, it is associated with the formation mechanism, the maturity, and the precursor of the gas. Therefore, PSIA provides a useful tool for determining the thermal maturity of thermogenic gases and their formation mechanisms. Although only a few studies have been conducted to date, PSIA of propane appears potentially useful in analyzing the origins and histories of natural hydrocarbons in geochemical settings (Piasecki et al., 2018; Suda et al., 2017). For

\* Corresponding author.

E-mail address: [xiongyq@gig.ac.cn](mailto:xiongyq@gig.ac.cn) (Y. Xiong).

example, the PSIA of propane in experimental and natural gas samples has shown that the position-specific carbon isotope composition of thermogenic propane correlates with thermal maturity; the dominant precursor (in order from kerogen to bitumen and finally to oil) correlates with a large increase ( $\sim 5\%$ ) in  $\delta^{13}\text{C}$  values of the central carbon of propane, thus suggesting the potential application of PSIA for differentiating gases generated from kerogen and bitumen (oil) (Piasecki et al., 2018). In addition, Suda et al. (2017) suggested the potential of using PSIA of carbon in propane to identify the different polymerization mechanisms of abiological hydrocarbons.

Various methods and techniques have been developed to measure intramolecular isotopic distributions, including quantitative  $^{13}\text{C}$  nuclear magnetic resonance (NMR) spectroscopy (Caer et al., 1991; Zhang et al., 1998, 1999; Caytan et al., 2007; Julien et al., 2015), ultra-high-resolution mass spectrometry (Eiler et al., 2013; Piasecki et al., 2016), and GC–IRMS measurements combined with off-line chemical and/or enzymatic degradation (Monson and Hayes, 1982; Gao et al., 2016) and on-line pyrolysis (Corso and Brenna, 1997; Dias et al., 2002). On-line pyrolysis coupled to GC–IRMS has been used to determine position-specific carbon isotopic compositions of various compounds, such as methyl palmitate (Corso and Brenna, 1997), alcohols (Corso et al., 1998), hydrocarbons (Corso and Brenna, 1999; Gilbert et al., 2016), acetic acid (Yamada et al., 2002; Hattori et al., 2011) and other low molecular weight organic acids (Dias et al., 2002), 3-methylthiopropylamine and isoamylamine (Sacks and Brenna, 2003), alaninol and phenethylamine (Wolyniak et al., 2005), propylene glycol (Wolyniak et al., 2006), and methyl tert-butyl ether (Gauchotte et al., 2009).

Propane is the simplest hydrocarbon molecule with an intramolecular isotope difference. Its position-specific carbon isotope distribution has been determined using high-resolution mass spectrometry (Piasecki et al., 2016), on-line pyrolysis coupled to GC–IRMS (Gilbert et al., 2016), and off-line enzymatic conversion combined with CSIA (Gao et al., 2016). However, high-resolution mass spectrometry requires an expensive IRMS instrument (e.g., Thermo IRMS 253 Ultra or Nu Panorama) and tedious separation of propane from natural gas (ca. 50  $\mu\text{mol}$  purified propane). Quantitative  $^{13}\text{C}$  NMR has low sensitivity and requires large sample sizes (tens to hundreds mmol). The off-line method suggested by Gao et al. (2016) is complicated and time consuming, and also requires a large volume of pure propane sample (8 mL). On-line pyrolysis coupled to GC–IRMS is rapid (generally less than one hour) and simple (no special purification, separation, or chemical transformation is required), and requires small samples (ca. 400 nmol). A method for determining the position-specific isotope composition of propane using on-line pyrolysis coupled to GC–IRMS has already been developed by Gilbert et al. (2016). This kind of system has been recently shown to work with propane from natural gas, and the C-scrambling associated with pyrolysis has been evaluated (Gilbert et al., 2016). Therefore, it was employed here to determine the intramolecular carbon isotope distribution of propane.

Conventional IRMS requires the conversion of analytes to  $\text{CO}_2$ , which loses intramolecular isotope information, making IRMS alone unsuitable for the intramolecular carbon isotope studies. Propane must first be quantitatively fragmented before GC–IRMS analysis. Several on-line pyrolysis systems have been developed for PSIA (Gauchotte-Lindsay and Turnbull, 2016). Although there is negligible exchange between C-atoms during pyrolysis (Gilbert et al., 2016), the  $\delta^{13}\text{C}$  values of the resulting fragments do not necessarily represent the position-specific  $\delta^{13}\text{C}$  values of the parent molecule, because isotope fractionation tends to alter the isotope relationship between the precursor and the fragments. Therefore, in addition to optimizing the pyrolysis conditions, various methods have been suggested to indirectly estimate the position-specific

isotope ratios from the measured fragment  $\delta^{13}\text{C}$  values. For example, the site preference (SP), defined as the difference of isotopic values between terminal and central C-atom positions, has been proposed as a way to evaluate the position-specific isotope fractionation of propane based on pyrolysis data and assumptions for isotopic fractionation (e.g., zero fractionation factors associated with the formation of methane and ethylene from propane) (Gilbert et al., 2016). The assumption of zero isotope fractionation associated with pyrolysis leads to systematic error in the determined SP values for propane. Although the estimated relative SP values can provide useful information, important information is still lost.

Although the C-scrambling associated with pyrolysis has been shown to be negligible (Gilbert et al., 2016), the isotope fractionation factors for pyrolysis reactions have not been evaluated. Here, we go one step further and provide a method to calculate the actual isotope fractionation factors in order to obtain absolute  $\delta^{13}\text{C}$  values for each position of propane. The main purpose of this study is to provide a method to calculate the absolute PSIA of propane using on-line pyrolysis coupled to GC–IRMS. The accuracy and precision of this method are evaluated.

## 2. Experimental

### 2.1. Samples

1- $^{13}\text{C}$ -enriched propane (isotopic enrichment 99.8%, purity 99.5%) (Sample A) was purchased from Cambridge Isotope Laboratories, Inc., USA. Propane with a natural carbon isotope abundance (purity 99.9%) (Sample B) was obtained from Jiehe Gas Inc., Gaoming, Foshan, Guangzhou, China, and was used to determine the optimal conditions of the pyrolysis experiment. In addition, three standard gas mixtures and two natural gases (Table 1) were analyzed to assess the method and determine average enrichment factors.

Because standards for intramolecular isotope analysis are not available, isotope-dilution experiments were used to evaluate the origin of fragments during propane pyrolysis (Sacks and Brenna, 2003) and the accuracy and precision of the on-line pyrolysis method (Dias et al., 2002). Six isotopically diluted samples of propane were prepared by spiking Sample A into Sample B. The dilution factors of each sample were 1486, 1839, 2900, 5730, 11,390, and no adding of Sample A (i.e., pure Sample B). The  $^{13}\text{C}$  distribution in the 2- and 3-C positions in Sample A is assumed to be homogeneous and representing the natural abundance (1.10%  $^{13}\text{C}$  and 98.90%  $^{12}\text{C}$ ; Tuli, 1985). Carbon isotope distribution in Sample B is also assumed to be homogenous. Therefore, the  $^{13}\text{C}/^{12}\text{C}$  ratio of

**Table 1**  
Information of gas samples used in this study.

Samples	Source information	Content of propane (v/v %)
1- $^{13}\text{C}$ -enriched propane (Sample A)	Cambridge Isotope Laboratories, Inc., USA	99.5
Propane (Sample B)	Jiehe gas, Inc., Foshan, Guangzhou, China	99.9
Standard Gas Mixture 1 (from Jiang Wenmin)	Jiehe gas, Inc., Foshan, Guangzhou, China	1.08
Standard Gas Mixture 2 (from Liu Jinzhong)	Hute gas, Inc., Foshan, Guangzhou, China	1.00
Standard Gas Mixture 3 (from Gao Shutao)	Beijing Hejinbeifen gas, Inc., Beijing, China	1.50
LH28-2-1 (2970.3 m)	Natural gas from China National Offshore Oil Corporation	19.07
LH28-2-1 (2854.2 m)	Natural gas from China National Offshore Oil Corporation	2.75

each carbon position is equal to that of Sample B and can be obtained from its relationship with the compound-specific isotope value measured by GC–IRMS. Because the dilution factors are >1000 in this experiment, the  $\delta^{13}\text{C}$  value of the central position in the isotope-dilution propane series is considered not to be affected by the addition of  $1\text{-}^{13}\text{C}$ -propane and is thus equal to the  $\delta^{13}\text{C}$  value of the central position of Sample B, while the  $^{13}\text{C}$  value of terminal positions in the diluted gas depends on the added amount of  $1\text{-}^{13}\text{C}$ -propane. The calculated  $^{13}\text{C}/^{12}\text{C}$  ratios of isotope-diluted propane are listed in Table 2.

## 2.2. On-line pyrolysis system

The system shown in Fig. 1 includes a GC, a laboratory-made pyrolysis furnace, and a conventional GC flame ionization detector (FID) and IRMS. The system of on-line pyrolysis coupled to GC–IRMS was developed following the work of Gilbert et al. (2016). Propane was isolated from natural gas on the first GC, which was equipped with a capillary column (HP-PLOT-Q, 30 m  $\times$  0.32 mm i. d., 20  $\mu\text{m}$  film thickness) and a two-position four-way valve. Propane eluted from the first GC column was switched to the high-temperature pyrolysis furnace by the four-way valve, where it underwent pyrolysis. A small length of deactivated fused silica capillary (0.32 mm i.d., Agilent) was used as a transfer line. The pyrolysis chamber was a resistively heated ceramic tube (32 cm  $\times$  0.55 mm i.d.), with temperature controlled to  $\pm 0.5$   $^{\circ}\text{C}$  by a Fe PXR-9 temperature controller (Fuji Electric, Japan). The pyrolysis fragments were separated by the second GC stage equipped with a capillary column (HP-PLOT-Q, 30 m  $\times$  0.32 mm i.d., 20  $\mu\text{m}$  film thickness), and then were introduced into a FID for composition analysis or IRMS for isotope measurement. The furnace and the second GC stage were connected via a deactivated fused silica capillary.

## 2.3. GC-pyrolysis (Py)-GC-FID analysis

The pure propane with natural carbon isotope abundance (Sample B) was diluted with nitrogen to a concentration of 1.56% prior to pyrolysis. Analysis by GC-Py-GC-FID determined the chemical composition of the pyrolysis products. First, 100  $\mu\text{L}$  of the diluted gas was introduced to the first GC stage (Agilent 7890) in each run, and six duplicate analyses were performed at each temperature point. The conditions of the first GC oven were as follows:

injection temperature 250  $^{\circ}\text{C}$ ; split ratio 10:1; flow rate 2.5 mL/min; oven temperature held at 50  $^{\circ}\text{C}$  for 5 min, ramped to 100  $^{\circ}\text{C}$  at 10  $^{\circ}\text{C}/\text{min}$ , then raised to 150  $^{\circ}\text{C}$  at 20  $^{\circ}\text{C}/\text{min}$ , and kept at 150  $^{\circ}\text{C}$  for 15 min. High-purity helium was used as the carrier gas. The second GC stage separated the pyrolytic products using the following temperature program: 40  $^{\circ}\text{C}$  constant for 10 min, then ramped to 190  $^{\circ}\text{C}$  at 20  $^{\circ}\text{C}/\text{min}$ , and kept at 190  $^{\circ}\text{C}$  for 5 min. The pyrolytic fragments were identified and quantified based on the retention times and response factors of two standard gas mixtures (Standard gas I:  $\text{CH}_4$  (v/v 5.12%),  $\text{C}_2\text{H}_6$  (v/v 2.01%),  $\text{C}_3\text{H}_8$  (v/v 1.08%),  $\text{C}_4\text{H}_{10}$  (v/v 1.00%),  $\text{C}_5\text{H}_{12}$  (v/v 1.01%), and  $\text{H}_2$  (v/v 1.21%) in helium; Standard gas II:  $\text{CH}_4$  (v/v 2.10%),  $\text{C}_2\text{H}_6$  (v/v 1.04%),  $\text{C}_2\text{H}_4$  (v/v 1.09%),  $\text{C}_3\text{H}_8$  (v/v 1.02%),  $\text{C}_3\text{H}_6$  (v/v 1.07%), and  $\text{H}_2$  (v/v 1.06%) in helium).

## 2.4. GC-Py-GC-IRMS analysis

GC-Py-GC-IRMS analysis was performed on the propane with natural isotope abundance (Sample B), a series of  $1\text{-}^{13}\text{C}$ -enriched propane samples diluted with Sample B, three standard gas mixtures, and two natural gases. The first GC oven was kept at 80  $^{\circ}\text{C}$  for 2 min, then raised to 190  $^{\circ}\text{C}$  at 20  $^{\circ}\text{C}/\text{min}$ , and held at 190  $^{\circ}\text{C}$  for 30 min. The split ratio was 5:1 for the analysis of the diluted Sample B and 30:1 for the diluted  $1\text{-}^{13}\text{C}$ -enriched propane series. Injection volumes of 150–600  $\mu\text{L}$  were used for the determination of Sample B diluted with nitrogen, and 50  $\mu\text{L}$  for the diluted  $1\text{-}^{13}\text{C}$ -enriched propane series. The oven program of the second GC was started at 35  $^{\circ}\text{C}$ , held for 10 min, ramped to 70  $^{\circ}\text{C}$  at 10  $^{\circ}\text{C}/\text{min}$ , then raised to 80  $^{\circ}\text{C}$  at 2  $^{\circ}\text{C}/\text{min}$ , and further heated to 190  $^{\circ}\text{C}$  at 20  $^{\circ}\text{C}/\text{min}$ , and kept at 190  $^{\circ}\text{C}$  for 10 min. The effluent was then introduced into a combustion furnace (operating at 850  $^{\circ}\text{C}$ ) and was converted to  $\text{CO}_2$ . Isotope ratios were calibrated against a working standard of  $\text{CO}_2$  gas ultimately calibrated against NIST RM-22 (graphite), and converted to delta notation given by the following equation:

$$\delta^{13}\text{C}_{\text{sample}} = (R_{\text{sample}}/R_{\text{PDB}} - 1) \times 1000 \quad (1)$$

where  $R = ^{13}\text{C}/^{12}\text{C}$ , and  $R_{\text{PDB}}$  is the isotope ratio of Pee Dee Belemnite, the international standard for carbon with  $^{13}\text{C}/^{12}\text{C} = 0.0112372$ .

The carbon isotopic compositions of pyrolytic products were determined on a GV IsoPrime stable isotope mass spectrometer. The reported isotopic data represent the arithmetic mean of at

**Table 2**

Calculated  $^{13}\text{C}/^{12}\text{C}$  ratios of the  $\alpha$ -position carbon of isotope-diluted propane and measured carbon isotope ratios of its pyrolytic fragments at 800, 820, and 840  $^{\circ}\text{C}$ .

Pyrolysis temperature ( $^{\circ}\text{C}$ )	Sample	Dilution factor	$^{13}\text{C}/^{12}\text{C}$ ratios					
			Parent $\text{C}_3\text{H}_8$	$\alpha$ -Position carbon	$\text{CH}_4$	$\text{C}_2\text{H}_4$	$\text{C}_2\text{H}_6$	$\text{C}_3\text{H}_6$
800	Isotope-dilution 1	1486	0.01112	0.01123	0.01119	0.01100	0.01109	0.01110
	Isotope-dilution 2	1839	0.01108	0.01117	0.01112	0.01097	0.01102	0.01105
	Isotope-dilution 3	2900	0.01101	0.01107	0.01102	0.01092	0.01092	0.01099
	Isotope-dilution 4	5730	0.01095	0.01098	0.01094	0.01087	0.01084	0.01093
	Isotope-dilution 5	11,390	0.01092	0.01094	0.01091	0.01086	0.01080	0.01091
	Pure sample B	–	0.01089	0.01089	0.01085	0.01083	0.01076	0.01088
820	Isotope-dilution 1	1486	0.01112	0.01123	0.01119	0.01101	0.01109	0.01111
	Isotope-dilution 2	1839	0.01108	0.01117	0.01113	0.01097	0.01103	0.01107
	Isotope-dilution 3	2900	0.01101	0.01107	0.01102	0.01092	0.01092	0.01100
	Isotope-dilution 4	5730	0.01095	0.01098	0.01095	0.01088	0.01084	0.01094
	Isotope-dilution 5	11,390	0.01092	0.01094	0.01092	0.01086	0.01081	0.01093
	Pure sample B	–	0.01089	0.01089	0.01086	0.01083	0.01076	0.01090
840	Isotope-dilution 1	1486	0.01112	0.01123	0.01120	0.01102	0.01111	0.01114
	Isotope-dilution 2	1839	0.01108	0.01117	0.01114	0.01099	0.01105	0.01110
	Isotope-dilution 3	2900	0.01101	0.01107	0.01103	0.01093	0.01094	0.01103
	Isotope-dilution 4	5730	0.01095	0.01098	0.01095	0.01089	0.01086	0.01097
	Isotope-dilution 5	11,390	0.01092	0.01094	0.01092	0.01087	0.01083	0.01095
	Pure sample B	–	0.01089	0.01089	0.01087	0.01084	0.01078	0.01092

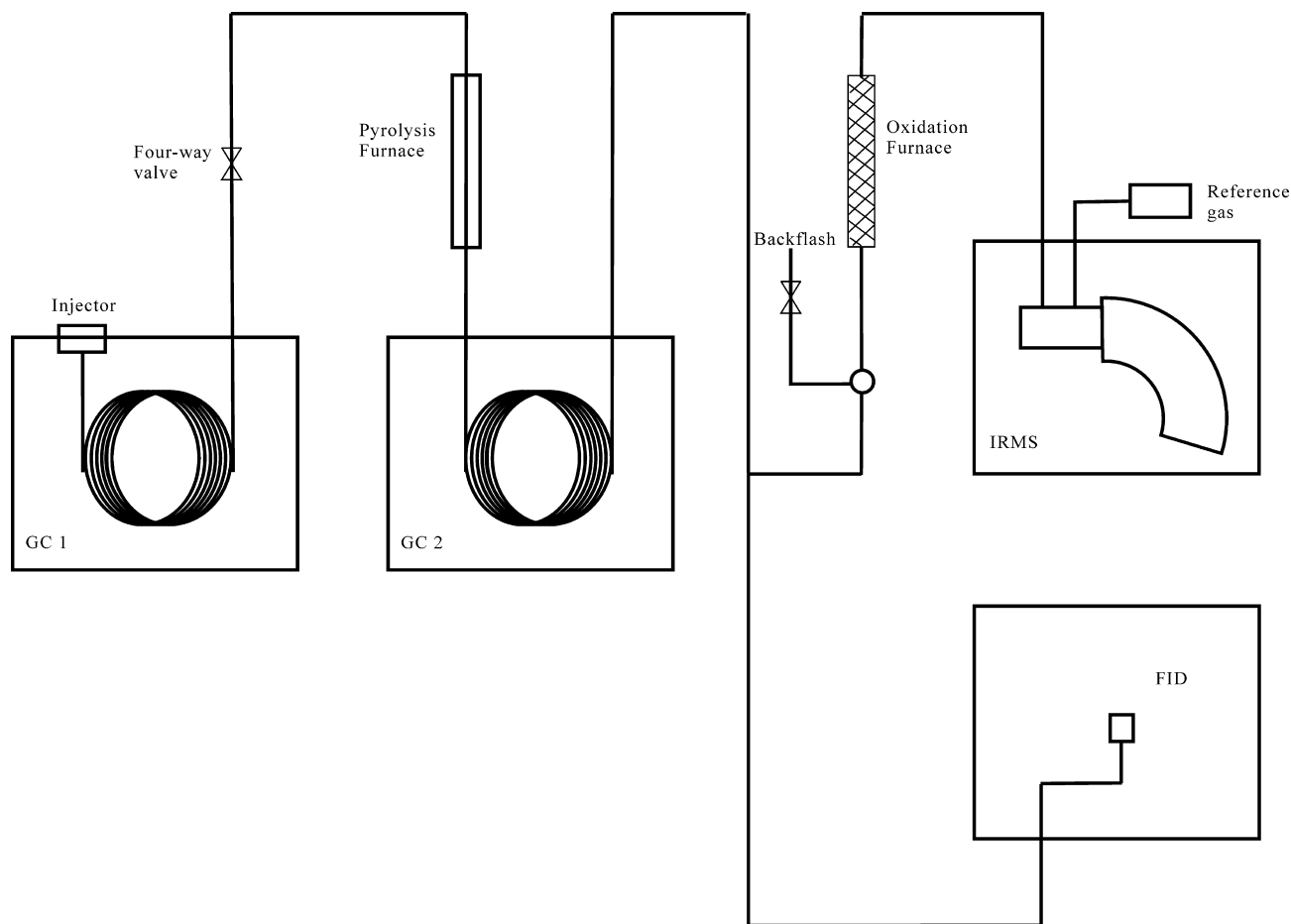


Fig. 1. Diagram of the on-line pyrolysis system.

least two duplicate analyses, and the standard deviation was less than 0.3‰.

### 3. Results

#### 3.1. Pyrolysis behavior of propane

Propane pyrolysis was performed at 660, 680, 700, 720, 740, 760, 780, 800, 820, 840, 860, 880, and 900 °C to understand its characteristics and establish optimal fragmentation conditions for PSIA. The representative gas chromatogram in Fig. 2 for propane pyrolyzed at 820 °C shows CH<sub>4</sub>, C<sub>2</sub>H<sub>4</sub>, C<sub>2</sub>H<sub>6</sub>, and C<sub>3</sub>H<sub>6</sub> as detected products. The percentage molar conversion (i.e., the molar ratio of a detected fragment to the parent compound injected on the column) was used here to assess the formation and decomposition of pyrolytic fragments. The molar conversions of pyrolytic fragments and the residual parent propane at different pyrolysis temperatures are shown in Fig. 3. The figure shows that once the propane pyrolysis temperature reached 720 °C, propane began to degrade and have a low fragmentation level (4.56%), with the pyrolysis fragments mainly comprising methane (CH<sub>4</sub>), ethylene (C<sub>2</sub>H<sub>4</sub>), and propylene (C<sub>3</sub>H<sub>6</sub>), and trace ethane (C<sub>2</sub>H<sub>6</sub>). Subsequently, at higher temperatures, propane fragmentation gradually increased, and the conversion of the pyrolytic products remarkably increased. When the pyrolysis temperature reached 840 and 880 °C the yields of C<sub>3</sub>H<sub>6</sub> and C<sub>2</sub>H<sub>6</sub> decreased, respectively, indicating that their degradation had exceeded their formation or that the reaction mechanism changed at those temperatures. In addition to CH<sub>4</sub>, C<sub>2</sub>H<sub>4</sub>, C<sub>2</sub>H<sub>6</sub>, and C<sub>3</sub>H<sub>6</sub>, a certain amount of acetylene

(C<sub>2</sub>H<sub>2</sub>), allene (C<sub>3</sub>H<sub>4</sub>), propyne (C<sub>3</sub>H<sub>4</sub>), and other heavier components were also detected at higher temperatures, suggesting that notable secondary reactions had occurred during pyrolysis.

To determine the effect of temperature on isotopic fractionation during pyrolysis, GC-Py-GC-IRMS analysis of the propane with diluted natural isotope abundance (Sample B) was conducted at 760–880 °C to induce differing degrees of fragmentation, with subsequent measurement of fragment isotope ratios. The isotopic composition of the residual propane increased with the pyrolysis temperature, consistent with increased propane decomposition (Fig. 4). The δ<sup>13</sup>C value of all the pyrolytic fragments showed the same evolution trend as propane: i.e., they all tended to be enriched in <sup>13</sup>C with increasing pyrolysis temperature. Pyrolysis below 800 °C resulted in no measurable δ<sup>13</sup>C value for C<sub>2</sub>H<sub>6</sub> due to the amount being below the limit of detection by IRMS analysis, and the δ<sup>13</sup>C values for CH<sub>4</sub> and C<sub>3</sub>H<sub>6</sub> showed relatively large errors due to their lower contents.

The pyrolytic results obtained here (Figs. 3 and 4) are consistent with those of Gilbert et al. (2016), suggesting that the pyrolysis is reproducible. Subtle differences between the two sets of results are probably due to the differences in the laboratory-made pyrolytic systems.

#### 3.2. Isotope-dilution experiments of propane

Isotope-dilution experiments were conducted to assess the origin of major fragments, including their original position on the parent molecule and the parent–daughter relationship between the pyrolytic fragments and propane. A series of isotope-diluted gases

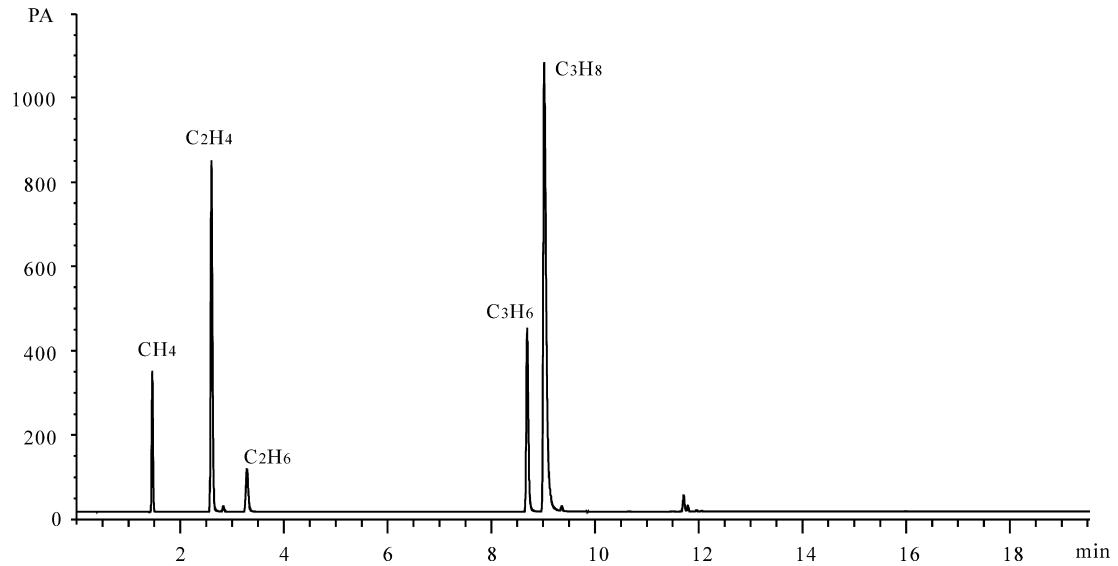


Fig. 2. Representative gas chromatogram of products from propane pyrolyzed at 820 °C.

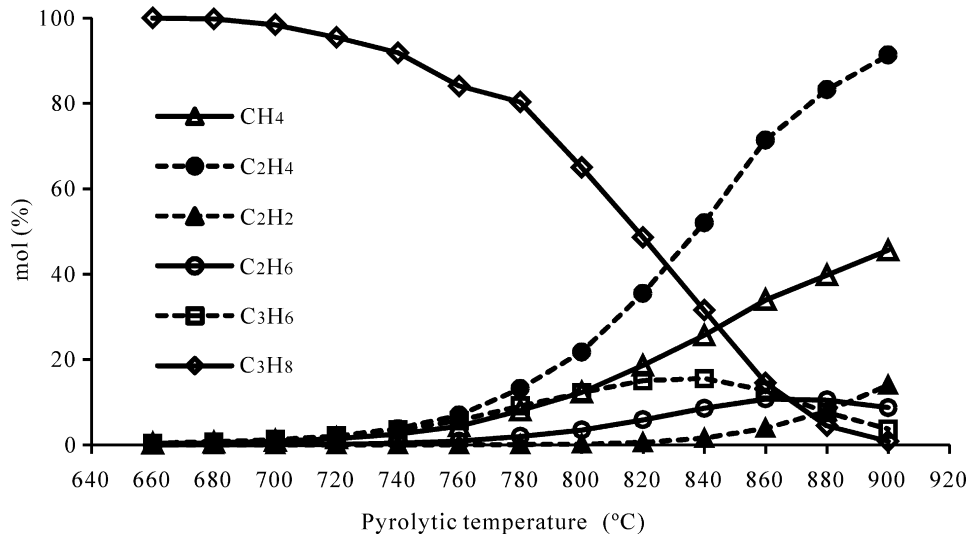


Fig. 3. Temperature dependence of molar conversion (mol%) of fragments and residual propane from propane pyrolysis.

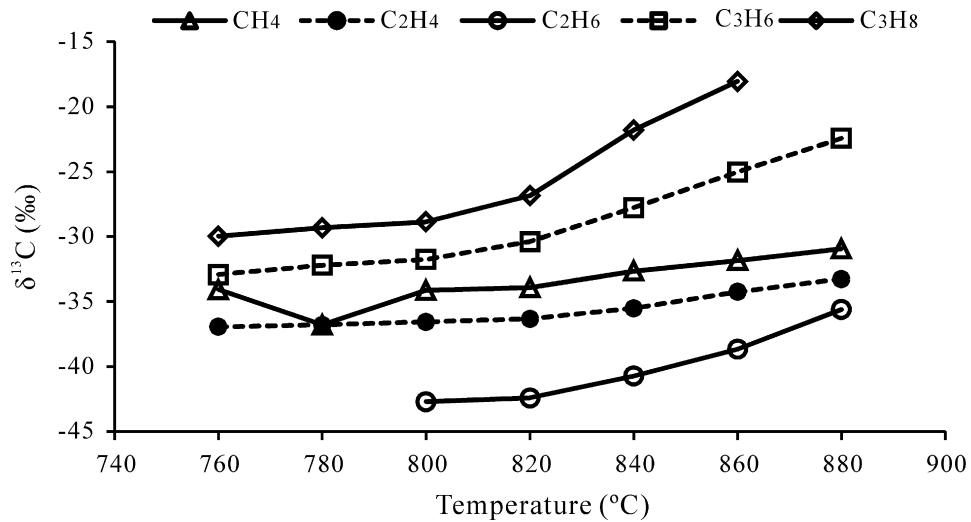


Fig. 4.  $\delta^{13}\text{C}$  values of residual propane and its pyrolytic fragments at different pyrolytic temperatures.

was prepared (Table 2), and pyrolysis experiments were performed at 800, 820, and 840 °C for each diluted sample. Carbon isotopic values of the fragments ( $\text{CH}_4$ ,  $\text{C}_2\text{H}_4$ ,  $\text{C}_2\text{H}_6$ , and  $\text{C}_3\text{H}_6$ ) were measured by GC-IRMS, and the corresponding carbon isotope ratios for each fragment ( $^{13}R_{\text{fragment}}$ ) are listed in Table 2. Isotope ratios of the terminal C-atom position in the parent propane ( $^{13}R_{a\text{-position}}$ ) were calculated (Table 2). Details of the calculation procedure are provided in Appendix A. Fig. 5 plots  $^{13}R_{\text{fragment}}$  with respect to  $^{13}R_{a\text{-position}}$

for the major fragments produced from the pyrolysis of the isotopically diluted gas series at 800, 820, and 840 °C, respectively. The relationship between  $^{13}R_{\text{fragment}}$  and  $^{13}R_{a\text{-position}}$  is used to investigate the origin of the pyrolytic fragments, which will be discussed in Section 4.2. The slopes of the linear regression equation  $^{13}R_{\text{fragment}} = f(^{13}R_{a\text{-position}})$  for  $\text{CH}_4$ ,  $\text{C}_2\text{H}_4$ ,  $\text{C}_2\text{H}_6$ , and  $\text{C}_3\text{H}_6$  at 820 °C are 96%, 51%, 96%, and 63%, respectively. Coefficients of determination  $r^2$  are all above 0.99.

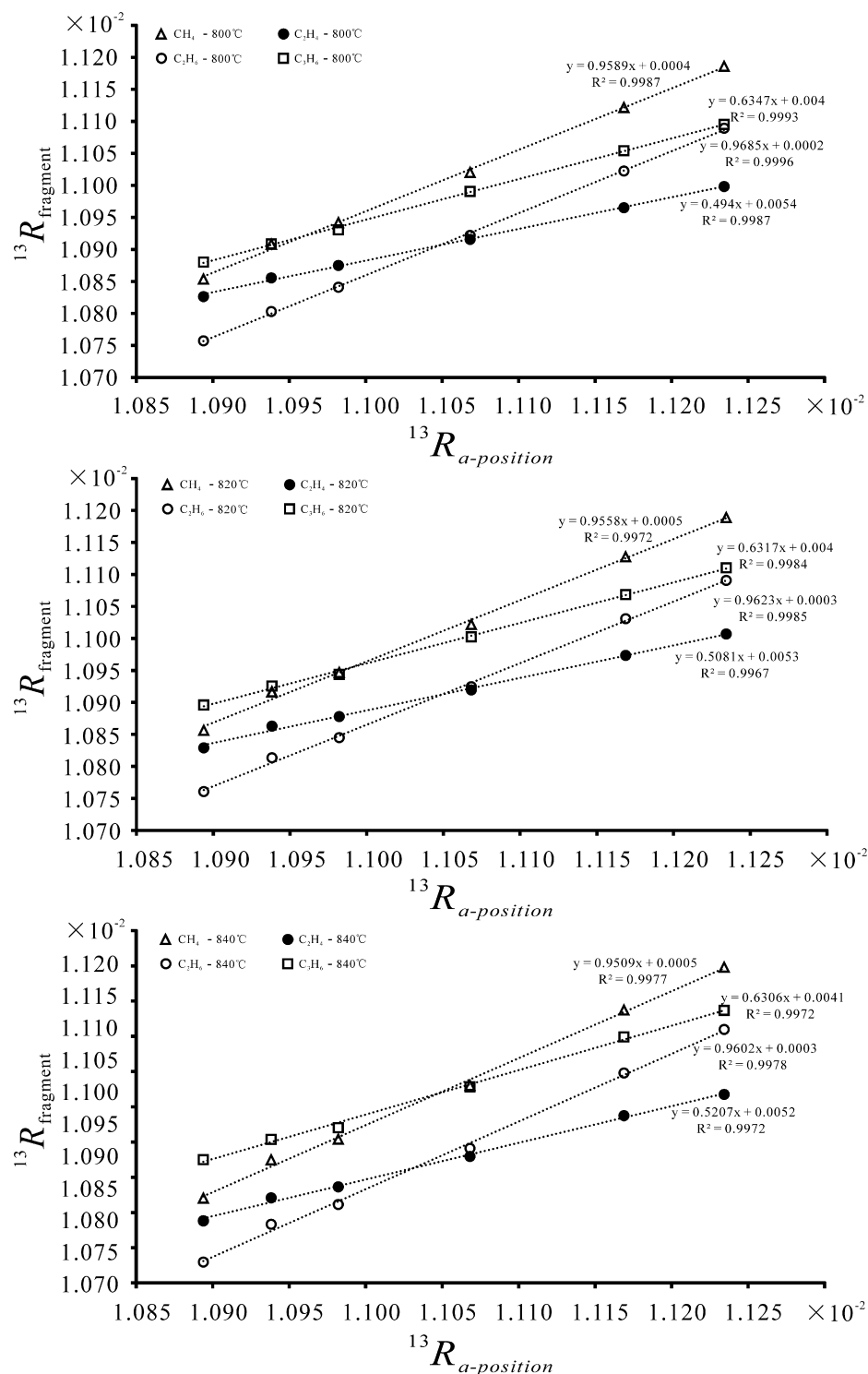


Fig. 5. Plots of  $^{13}R_{\text{fragment}}$  versus  $^{13}R_{a\text{-position}}$  for the major fragments produced from the pyrolysis of isotopically diluted gas series at 800, 820, and 840 °C, respectively.

## 4. Discussion

This study used on-line pyrolysis coupled to GC–IRMS to determine the position-specific carbon isotope composition of propane in natural gas. Ideally, the method is based on three conditions: (a) Carbon isotope fractionation related to pyrolysis must be quantitatively evaluated; (b) The relationship between the pyrolytic fragments and propane must be clear. Secondary reactions should be negligible; (c) The amounts of pyrolytic products must be high enough to meet the requirements of GC–IRMS analysis.

### 4.1. Optimization of pyrolysis temperature

Accurate determination of the position-specific carbon isotope composition of propane based on artificial pyrolysis relies on two factors: secondary reactions must be minimized and there must be sufficient pyrolytic fragments for accurate GC–IRMS measurement. These requirements conflict, so choosing the optimal pyrolysis temperature requires compromise. Data in Fig. 3 show that the fragmentation pattern of propane changed when the pyrolysis temperature reached 840 °C, as the yield of C<sub>3</sub>H<sub>6</sub> started to decrease and a certain amount of C<sub>2</sub>H<sub>2</sub> began to be detected, both suggesting the presence of secondary reactions. Therefore, 840 °C is considered as the upper temperature limit of pyrolysis for PSIA to minimize secondary reactions. Fig. 4 shows that the δ<sup>13</sup>C value for C<sub>2</sub>H<sub>6</sub> cannot be measured when the pyrolysis temperature is below 800 °C, owing to the amount being below the limit of detection by IRMS analysis. Therefore, 800 °C was considered as the lower temperature limit for pyrolysis in this study, and we concluded that 800–840 °C is the optimal propane pyrolysis temperature range for PSIA in our experimental arrangement.

### 4.2. Origin of pyrolytic fragments

Once the appropriate range of pyrolysis temperatures was established, isotope-dilution experiments were performed to assess the origin of major fragments. According to the suggestion by Sacks and Brenna (2003), the measured isotope ratio of a fragment can be expressed as a weighted sum of the isotope ratios from each carbon position:

$$^{13}R_{\text{fragment}} = ^{13}R_{a\text{-position}}X_{a\text{-position}} + ^{13}R_{b\text{-position}}X_{b\text{-position}}, \quad (2)$$

where  $^{13}R_{\text{fragment}}$  is the measured isotope ratio of a fragment,  $^{13}R_{a\text{-position}}$  and  $^{13}R_{b\text{-position}}$  are the isotope ratios of terminal and central C-atom positions in the parent propane, respectively, and  $X_{a\text{-position}}$  and  $X_{b\text{-position}}$  are the molar fractions that the corresponding positions contribute to the fragment, respectively. The slope of  $^{13}R_{\text{fragment}} = f(^{13}R_{a\text{-position}})$  for each fragment in Fig. 5 represents the fractional contribution of the labeled position (a-position) to the fragment, i.e., the fidelity of the labeled carbon position for the fragment (Wolyniak et al., 2006). Isotope labeling experiments showed that pyrolytic fragments should ideally originate from unique sites within the parent propane molecule. For example, the slopes of the best-fit lines for CH<sub>4</sub>, C<sub>2</sub>H<sub>4</sub>, C<sub>2</sub>H<sub>6</sub>, and C<sub>3</sub>H<sub>6</sub> at 820 °C are 96%, 51%, 96%, and 63%, respectively, indicating that CH<sub>4</sub> and C<sub>2</sub>H<sub>6</sub> are derived entirely from the terminal methyl carbon, while ~50% of C<sub>2</sub>H<sub>4</sub> and about two thirds of C<sub>3</sub>H<sub>6</sub> are derived from the terminal positions of propane. That C<sub>2</sub>H<sub>6</sub> originated with 96% fidelity from the terminal carbon indicating that it resulted from the recombination of methyl free radicals. The approximately two-thirds of C<sub>3</sub>H<sub>6</sub> derived from the terminal position of propane suggests that C<sub>3</sub>H<sub>6</sub> formed by the dehydration of propane. The fractions of terminal carbons of propane in CH<sub>4</sub> and C<sub>2</sub>H<sub>4</sub> indicate that CH<sub>4</sub> and C<sub>2</sub>H<sub>4</sub> were generated through the single C–C bond breaking of propane or propene. Ideal fidelity of the labeled terminal position for the pyrolysis frag-

ments (CH<sub>4</sub>, C<sub>2</sub>H<sub>4</sub>, C<sub>2</sub>H<sub>6</sub>, and C<sub>3</sub>H<sub>6</sub>) also indicates that there was no significant exchange of C-atoms during pyrolysis, which is consistent with the conclusion of Gilbert et al. (2016). Therefore, isotope ratios of the terminal and central positions within propane appear to be obtainable from the fragment isotope ratios. In addition, Fig. 5 shows the slopes of the best-fit lines for CH<sub>4</sub>, C<sub>2</sub>H<sub>4</sub>, C<sub>2</sub>H<sub>6</sub>, and C<sub>3</sub>H<sub>6</sub> at 800 and 840 °C as being close to the corresponding values at 820 °C (i.e. 96%, 49%, 97%, and 63% at 800 °C and 95%, 52%, 96%, and 63% at 840 °C, respectively), indicating the pyrolytic behavior of propane at 800–840 °C to be stable, and thus that this range of temperatures is suitable for the PSIA study in present work.

### 4.3. Kinetic isotope effect associated with position-specific C-atoms of propane pyrolysis

Most natural propane is generated from the cracking of sedimentary organic matter, but the precise mechanisms remain unclear. Previous studies have indicated that propane pyrolysis is not simple C–C bond breaking leading to the formation of CH<sub>4</sub> and C<sub>2</sub>H<sub>4</sub>, but rather an entirely free-radical reaction (Layokun and Slater, 1979). The key initiation step is



followed by a series of chain-propagation and chain-termination reactions (Layokun and Slater, 1979). Thus, propane cracking is a complex process that includes many reactions, some of which have not been investigated even with labeled experiments. In the present study, as shown in Fig. 6, the complex reaction process is represented by at least three pseudo-reactions: C–C bond cleavage into methane and ethylene, dehydrogenation of propane to propylene, and formation of ethane through recombination of methyl radicals. One pseudo-reaction does not represent a real reaction process, but may represent the overall result of a series of reactions. For example, the reactions by which propane forms propylene, which then directly forms ethylene and methane, can be included in the pseudo-reaction that propane forms ethylene and methane. Therefore, the isotope fractionations relating to both the <sup>13</sup>C-depleted propylene and the <sup>13</sup>C-enriched remaining propane have been included in the total fractionation of the pseudo-reaction: i.e., C–C bond cleavage into methane and ethylene.

GC–IRMS only determines isotope ratios at the compound-specific level, and thus cannot obtain fractionation factors for each site. As the pyrolysis of propane is not complete at 820–840 °C, pyrolysis-induced isotopic fractionation will occur, and absolute PSIA data cannot be directly determined. Relative PSIA values can be calculated by arbitrarily selecting a sample as a standard and setting its isotope ratios at each position to zero; these can then be used to compare the isotopic variation at a single position within the parent molecule (Wolyniak et al., 2005). Using propylene glycol as a model compound, a method that quantified isotopic fractionation during pyrolysis was suggested to calculate absolute isotope ratios for each position (Wolyniak et al., 2006).

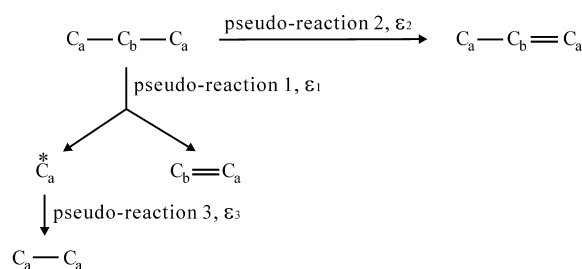


Fig. 6. Schematic view of the major reactions during the pyrolysis of propane. Modified from Gilbert et al. (2016).

The measured  $^{13}\text{C}/^{12}\text{C}$  ratios of fragments depend on the position-specific carbon isotopic composition of propane and isotope fractionation factors associated with its pyrolysis. However, in contrast with the assumption that only a single isotope enrichment factor is applicable for each position (Wolyniak et al., 2006), different isotope enrichment factors were assumed for each major reaction in this study (Fig. 6).

Transformation of methyl radicals into ethane will lead to the existing  $\text{CH}_4$  becoming enriched in  $^{13}\text{C}$ . The effect of this reaction can be corrected based on the amount and  $\delta^{13}\text{C}$  values of  $\text{CH}_4$  and  $\text{C}_2\text{H}_6$ . Thus, the original  $\delta^{13}\text{C}$  value of  $\text{CH}_4$  (including C-atoms of  $\text{C}_2\text{H}_6$ ) can be calculated by using a mass balance.

$$\delta^{13}\text{C}_{\text{CH}_4, \text{corrected}} = (m_{\text{CH}_4} \times \delta^{13}\text{C}_{\text{CH}_4} + 2m_{\text{C}_2\text{H}_6} \times \delta^{13}\text{C}_{\text{C}_2\text{H}_6}) / (m_{\text{CH}_4} + 2m_{\text{C}_2\text{H}_6}), \quad (4)$$

where  $m_{\text{CH}_4}$  and  $m_{\text{C}_2\text{H}_6}$  are the molar yields of pyrolysis fragments  $\text{CH}_4$  and  $\text{C}_2\text{H}_6$  (data in Fig. 3), respectively, and  $\delta^{13}\text{C}_{\text{CH}_4}$  and  $\delta^{13}\text{C}_{\text{C}_2\text{H}_6}$  are the carbon isotope compositions of  $\text{CH}_4$  and  $\text{C}_2\text{H}_6$ , respectively. Based on the origin of the pyrolysis fragments from propane, their carbon isotope ratios can be expressed by the following equations:

$$\delta^{13}\text{C}_{\text{CH}_4, \text{corrected}} = \delta^{13}\text{C}_a + \varepsilon_1, \quad (5)$$

$$\delta^{13}\text{C}_{\text{C}_2\text{H}_4} = (\delta^{13}\text{C}_a + \delta^{13}\text{C}_b + \varepsilon_1) / 2, \quad (6)$$

$$\delta^{13}\text{C}_{\text{C}_3\text{H}_6} = (2\delta^{13}\text{C}_a + \delta^{13}\text{C}_b) / 3 + \varepsilon_2, \quad (7)$$

$$\delta^{13}\text{C}_{\text{C}_2\text{H}_6} = \delta^{13}\text{C}_a + \varepsilon_1 + \varepsilon_3, \quad (8)$$

where  $\delta^{13}\text{C}_{\text{C}_2\text{H}_4}$ ,  $\delta^{13}\text{C}_{\text{C}_2\text{H}_6}$ , and  $\delta^{13}\text{C}_{\text{C}_3\text{H}_6}$  are the carbon isotope compositions of the pyrolysis fragments ( $\text{C}_2\text{H}_4$ ,  $\text{C}_2\text{H}_6$ , and  $\text{C}_3\text{H}_6$ , respectively).  $\delta^{13}\text{C}_a$  and  $\delta^{13}\text{C}_b$  represent the initial carbon isotope values of the terminal methyl carbons and the central methylene carbon of propane, respectively.  $\varepsilon_1$ ,  $\varepsilon_2$ , and  $\varepsilon_3$  are the overall carbon isotope enrichment factors associated with the three major reactions shown in Fig. 6, and depend on the pyrolysis temperature (and thus remain constant at a certain temperature). The  $\delta^{13}\text{C}$  values of these pyrolytic products and the original reactant can be determined. Mass balance leads to

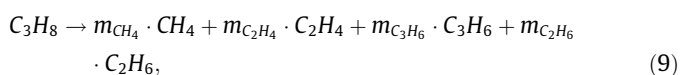


**Table 3**  
 $\delta^{13}\text{C}$  values of pyrolytic fragments of propane in six gas samples pyrolyzed at 820 °C.

Pyrolytic fragments	$\delta^{13}\text{C}$ values (‰)					
	Sample B (n = 5)	Standard gas mixture 1 (n = 4)	Standard gas mixture 2 (n = 5)	Standard gas mixture 3 (n = 4)	LH28-2-1 (2970.3 m) (n = 4)	LH28-2-1 (2854.2 m) (n = 4)
$\text{CH}_4$	$-33.9 \pm 0.14$	$-33.5 \pm 0.08$	$-35.1 \pm 0.12$	$-35.4 \pm 0.15$	$-23.9 \pm 0.15$	$-26.8 \pm 0.20$
$\text{C}_2\text{H}_4$	$-36.3 \pm 0.16$	$-33.0 \pm 0.11$	$-37.6 \pm 0.06$	$-37.6 \pm 0.15$	$-26.9 \pm 0.04$	$-29.3 \pm 0.11$
$\text{C}_2\text{H}_6$	$-42.4 \pm 0.19$	$-41.9 \pm 0.34$	$-42.0 \pm 0.23$	$-43.7 \pm 0.23$	$-32.2 \pm 0.16$	$-35.2 \pm 0.22$
$\text{C}_3\text{H}_6$	$-30.4 \pm 0.29$	$-27.3 \pm 0.20$	$-31.7 \pm 0.15$	$-31.3 \pm 0.30$	$-20.4 \pm 0.31$	$-22.8 \pm 0.26$

**Table 4**  
Calculated enrichment factors and absolute  $\delta^{13}\text{C}$  values of position-specific carbons of propane.

Samples	$\varepsilon_1$ (‰)	$\varepsilon_2$ (‰)	$\varepsilon_3$ (‰)	a (‰)	b (‰)	Calculated $\delta^{13}\text{C}_{\text{propane}}$ (‰)	Measured $\delta^{13}\text{C}_{\text{propane}}$ (‰)	Deviation <sup>a</sup> (‰)
Sample B	-9.2	0.1	-5.2	-28.0	-35.4	-30.5	-30.6	0.1
Standard gas mixture 1	-9.0	0.9	-4.6	-27.7	-29.4	-28.3	-28.3	0.0
Standard gas mixture 2	-8.8	0.1	-4.2	-29.0	-37.3	-31.8	-31.9	0.1
Standard gas mixture 3	-8.1	1.3	-5.1	-30.5	-36.6	-32.5	-32.6	0.1
LH28-2-1 (2970.3 m)	-8.7	0.8	-5.1	-18.4	-26.6	-21.1	-21.2	0.1
LH28-2-1 (2854.2 m)	-9.3	0.5	-5.1	-20.8	-28.5	-23.4	-23.5	0.1
Average value	$-8.9 \pm 0.4$	$-0.6 \pm 0.4$	$-4.9 \pm 0.4$	-	-	-	-	-

<sup>a</sup> Deviation = Calculated  $\delta^{13}\text{C}_{\text{propane}}$  - Measured  $\delta^{13}\text{C}_{\text{propane}}$ .

where  $m_{\text{CH}_4}$ ,  $m_{\text{C}_2\text{H}_4}$ ,  $m_{\text{C}_3\text{H}_6}$ , and  $m_{\text{C}_2\text{H}_6}$  are the molar yields of pyrolysis fragments  $\text{CH}_4$ ,  $\text{C}_2\text{H}_4$ ,  $\text{C}_3\text{H}_6$ , and  $\text{C}_2\text{H}_6$ , respectively (data in Fig. 3). The mass fraction of carbon content  $X_i$  for fragment  $i$  in the pyrolytic products can be calculated by the following equation:

$$X_i = \frac{m_i \cdot n_i}{\sum m_i \cdot n_i} = \frac{m_i \cdot n_i}{m_{\text{CH}_4} + m_{\text{C}_2\text{H}_4} \cdot 2 + m_{\text{C}_2\text{H}_6} \cdot 2 + m_{\text{C}_3\text{H}_6} \cdot 3}, \quad (10)$$

where  $n_i$  is the number of carbon atoms in fragment  $i$ . Therefore, according to the equations suggested by Wolyniak et al. (2006), the  $\delta^{13}\text{C}$  value of pyrolyzed propane can be calculated using the following weighted sum.

$$\delta^{13}\text{C}_{\text{C}_3\text{H}_8, \text{pyrolyzed}} = (X_{\text{CH}_4} \cdot \delta^{13}\text{C}_{\text{CH}_4} + X_{\text{C}_2\text{H}_4} \cdot \delta^{13}\text{C}_{\text{C}_2\text{H}_4} + X_{\text{C}_2\text{H}_6} \cdot \delta^{13}\text{C}_{\text{C}_2\text{H}_6} + X_{\text{C}_3\text{H}_6} \cdot \delta^{13}\text{C}_{\text{C}_3\text{H}_6}). \quad (11)$$

The total fractionation ( $\Delta^{13}\text{C}$ ) is the difference between the  $\delta^{13}\text{C}$  value of the parent and  $\delta^{13}\text{C}_{\text{C}_3\text{H}_8, \text{pyrolyzed}}$  (i.e.,  $\delta^{13}\text{C}_{\text{C}_3\text{H}_8, \text{pyrolyzed}} - \delta^{13}\text{C}_{\text{C}_3\text{H}_8, \text{original}}$ ), and can also be calculated by site-specific fractionation.

$$\Delta^{13}\text{C} = (X_{\text{CH}_4} + X_{\text{C}_2\text{H}_6}) \cdot \varepsilon_1 + X_{\text{C}_2\text{H}_4} \cdot \varepsilon_1 / 2 + X_{\text{C}_3\text{H}_6} \cdot \varepsilon_2. \quad (12)$$

For pyrolysis at 820 °C of propane with natural  $^{13}\text{C}$  abundance (Sample B), Eqs. (4)–(12) and the data in Table 3 give calculated results of  $\varepsilon_1 = -9.2\text{‰}$ ,  $\varepsilon_2 = 0.1\text{‰}$ , and  $\varepsilon_3 = -5.2\text{‰}$ . Details of the calculation procedure are provided in Appendix B. The corresponding calculated values of  $\delta^{13}\text{C}_a$  and  $\delta^{13}\text{C}_b$  are listed in Table 4.

Table 5 shows good consistency of  $\delta^{13}\text{C}_a$  and  $\delta^{13}\text{C}_b$  values measured at 800–840 °C for Sample B, indicating that this range is suitable for the determination of position-specific carbon isotope composition in this study. To improve the yield of pyrolysate while minimizing secondary reactions, pyrolysis was conducted at 820 °C in the following experiment.

#### 4.4. Determination of position-specific $\delta^{13}\text{C}$ values and $^{13}\text{C}$ site preference in propane

Similarly, three standard gas mixtures and two natural gases were analyzed to find the PSIA of propane. As the original compound-specific  $\delta^{13}\text{C}$  values of the labeled samples have not been measured in the present study, the  $\varepsilon$  values cannot be obtained without the original compound-specific  $\delta^{13}\text{C}$  value of the parent propane, and the labeled samples are not included in



**Table 5**

Calculated enrichment factors and absolute  $\delta^{13}\text{C}$  values of position-specific carbons of propane in Sample B, pyrolyzed at 800, 820, and 840 °C.

Pyrolytic temperature (°C)	Parameter values (‰)				
	$\varepsilon_1$	$\varepsilon_2$	$\varepsilon_3$	a	b
800	-9.5	-1.3	-5.5	-27.8	-35.9
820	-9.2	0.1	-5.2	-28.0	-35.4
840	-7.8	2.7	-4.8	-28.1	-35.1

the discussion. The calculated results are also listed in Table 4, and the average values of  $\varepsilon_1$ ,  $\varepsilon_2$  and  $\varepsilon_3$  were obtained from all six samples. Values for  $\varepsilon_1$ ,  $\varepsilon_2$ , and  $\varepsilon_3$  showed relatively low deviation (<0.5‰), indicating that the isotope enrichment factor related to each reaction at a certain temperature is stable and is independent of the character of the sample. Therefore, the average values of  $\varepsilon_1$ ,  $\varepsilon_2$ , and  $\varepsilon_3$  were considered as the enrichment factors relating to the three major reactions at 820 °C in this system, and thus can be used in future determinations.

The SP value for propane can be calculated using the following equation deduced from Eqs. (5) and (6):

$$\text{SP} = \delta^{13}\text{C}_a - \delta^{13}\text{C}_b = (\delta^{13}\text{C}_{\text{CH}_4, \text{corrected}} - \delta^{13}\text{C}_{\text{C}_2\text{H}_4}) \times 2 - \varepsilon_1. \quad (13)$$

Therefore, there is a systematic deviation of SP,  $-\varepsilon_1$  (which is ca. 8.9‰ for propane pyrolysis at 820 °C), between the values from this study and that of Gilbert et al. (2016).

Values for  $\delta^{13}\text{C}_a$  and  $\delta^{13}\text{C}_b$  can also be calculated by the following equations derived from Eqs. (5) and (6):

$$\delta^{13}\text{C}_a = \delta^{13}\text{C}_{\text{CH}_4, \text{corrected}} - \varepsilon_1, \quad (14)$$

$$\delta^{13}\text{C}_b = 2 \times \delta^{13}\text{C}_{\text{C}_2\text{H}_4} - \delta^{13}\text{C}_{\text{CH}_4, \text{corrected}}. \quad (15)$$

Therefore, we can obtain position-specific  $\delta^{13}\text{C}$  values and the SP value of propane from the measured  $\delta^{13}\text{C}$  values of the  $\text{CH}_4$ ,  $\text{C}_2\text{H}_4$ ,  $\text{C}_2\text{H}_6$ , and  $\text{C}_3\text{H}_6$  fragments according to Eqs. (13)–(15). The CSIA value of propane ( $\delta^{13}\text{C}_{\text{propane}}$ ) is an average of the PSIA values of two a-position carbons ( $\delta^{13}\text{C}_a$ ) and one b-position carbon ( $\delta^{13}\text{C}_b$ ): i.e.,  $\delta^{13}\text{C}_{\text{C}_3\text{H}_8} = (2\delta^{13}\text{C}_a + \delta^{13}\text{C}_b)/3$ . As shown in Table 4, the calculated  $\delta^{13}\text{C}_{\text{propane}}$  values based on the PSIA data are consistent with the measured  $\delta^{13}\text{C}_{\text{propane}}$  values of initial propane prior to pyrolysis (deviation <0.3‰, determination error of GC-IRMS; Table 4), indicating that the position-specific carbon isotope composition determined here is relatively accurate.

For the GC-IRMS analysis, the limit of quantification is ~10 ng of carbon on the column to achieve a standard deviation value within <0.5‰. The fragment of propane pyrolysis present in the lowest amount is  $\text{C}_2\text{H}_6$ , which forms with a molar conversion of 5.9% at 820 °C, and thus requires ~7.1 nmol of propane for quantification.

## 5. Conclusions

On-line pyrolysis coupled with GC-IRMS was used to determine the position-specific carbon isotope ratio of propane in natural gas. The results indicate that the origin position of pyrolytic fragments can be identified for a series of isotope-dilution gases prepared by adding isotopically labeled propane ( $1\text{-}^{13}\text{C}$ -enriched propane) into a propane sample with natural  $^{13}\text{C}$  abundance. The carbon isotopic enrichment factors associated with propane pyrolysis were calculated from the measured  $\delta^{13}\text{C}$  values of the pyrolytic fragments. The absolute  $\delta^{13}\text{C}$  values for position-specific carbon in propane and its  $^{13}\text{C}$  SP value can be calculated based on the  $\delta^{13}\text{C}$  values and enrichment factors of  $\text{CH}_4$ ,  $\text{C}_2\text{H}_4$ ,  $\text{C}_3\text{H}_6$ , and  $\text{C}_2\text{H}_6$  fragments.

## Acknowledgements

This work was supported by the National Natural Science Foundation of China (Grant numbers 41773034 and 41372138); the Strategic Priority Research Program of the Chinese Academy of Sciences (Grant number XDA14010102); and the Self-Research Foundation of State Key Laboratory of Organic Geochemistry, Guangzhou Institute of Geochemistry, Chinese Academy of Sciences (Grant number SKLOG2016-A07). This is contribution IS-2052 from GIGCAS. We acknowledge A.R. Gilbert, B. Bernard, and the Associate Editor J.A. Curiale as reviewers of the paper, and Editor-in-Chief John Volkman for editorial and technical assistance.

## Appendix A. Calculation of values of $^{13}\text{R}_a$ -position listed in Table 2

First, the  $^{13}\text{C}/^{12}\text{C}$  ratios of Sample A and Sample B were calculated. The  $^{13}\text{C}$  distribution in the 2- and 3-C positions of Sample A was assumed to be homogeneous and representative of the natural abundance (i.e., 1.10%  $^{13}\text{C}$  and 98.90%  $^{12}\text{C}$ ; Tuli, 1985). Thus, the  $^{13}\text{C}/^{12}\text{C}$  ratio of Sample A ( $R_A$ ) could be calculated as follows (note that the equation numbering differs to that in the main text):

$$R_A = \frac{\delta^{13}\text{C}_A}{\delta^{12}\text{C}_A} = \frac{1 \times 100\% + 2 \times 1.10\%}{0 \times 100\% + 2 \times 98.90\%} = 0.516684. \quad (A.1)$$

The compound-specific  $\delta^{13}\text{C}$  value of Sample B ( $\delta^{13}\text{C}_B$ ) was determined by GC-IRMS to be  $-30.55\%$ , and the calculated value of  $R_B$  is 0.0108939 according to the following equation:

$$R = \left( \frac{\delta^{13}\text{C}}{1000} + 1 \right) \times R_{\text{PDB}}, \quad (A.2)$$

where  $R_{\text{PDB}}$  is 0.0112372.

The  $^{13}\text{C}/^{12}\text{C}$  ratio of isotope-diluted propane was then calculated. Sample A was diluted with Sample B, and the dilution factors of the isotope-diluted propane samples listed in Table 2 were determined based on their volumes. Assuming that the volume ratio of A:B in the isotope-diluted sample is X:1 (the value of X is equal to  $1/(\text{dilution factor} - 1)$ ), then the  $^{13}\text{C}/^{12}\text{C}$  ratios of the isotopically diluted samples (i.e., parent  $\text{C}_3\text{H}_8$  in Table 2) were calculated as follows:

$$\delta^{13}\text{C}_X = \left( \frac{R_A}{1 + R_A} \right) \times X + \left( \frac{R_B}{1 + R_B} \right) \times 1, \quad (A.3)$$

$$\delta^{12}\text{C}_X = \left( \frac{1}{1 + R_A} \right) \times X + \left( \frac{1}{1 + R_B} \right) \times 1, \quad (A.4)$$

$$R_X = \frac{\delta^{13}\text{C}_X}{\delta^{12}\text{C}_X} = \frac{R_B \times (1 + R_A) + R_A \times (1 + R_B) \times X}{(1 + R_A) + (1 + R_B) \times X}, \quad (A.5)$$

where  $^{13}\text{C}_X$  and  $^{12}\text{C}_X$  are the concentrations of  $^{13}\text{C}$  and  $^{12}\text{C}$  in the isotope-diluted samples, and  $R_X$  is the  $^{13}\text{C}/^{12}\text{C}$  ratio of the isotope-diluted propane.

As stated in the main text, "Because the dilution factors are above 1000 in this experiment, the  $\delta^{13}\text{C}$  value of the central position ( $\delta^{13}\text{C}_b$ ) in the isotope-diluted propane series is considered not to be affected by the addition of  $1\text{-}^{13}\text{C}$ -propane, and is thus equal to the  $\delta^{13}\text{C}$  value of the central position of Sample B". Therefore, the  $\delta^{13}\text{C}$  value of the central position in the isotope-diluted propane series is  $-30.55\%$ . Thus, the  $^{13}\text{C}/^{12}\text{C}$  ratio of the central carbon ( $R_b$ ) is 0.0108939.

We know that

$$\delta^{13}\text{C}_X = \frac{2}{3} \times \delta^{13}\text{C}_a + \frac{1}{3} \times \delta^{13}\text{C}_b, \quad (A.6)$$

where  $\delta^{13}\text{C}_X$  is the compound-specific  $\delta^{13}\text{C}$  value of the isotope-diluted sample, which can be determined by IRMS directly; and

$\delta^{13}C_a$  and  $\delta^{13}C_b$  represent the  $\delta^{13}C$  values of the terminal position (a-position) and central position (b-position), respectively, in the isotope-diluted propane. Therefore, the  $^{13}C/^{12}C$  ratio of the a-position ( $R_a$ ) can be deduced from Eqs. (A.6) and (A.2).

## Appendix B. Calculation of $\epsilon$ values

The  $\epsilon$  values were calculated using the following five equations.

$$\delta^{13}C_{CH_4,corrected} = \delta^{13}C_a + \epsilon_1 \quad (A.7)$$

$$\delta^{13}C_{C_2H_4} = (\delta^{13}C_a + \delta^{13}C_b + \epsilon_1)/2 \quad (A.8)$$

$$\delta^{13}C_{C_3H_6} = (2\delta^{13}C_a + \delta^{13}C_b)/3 + \epsilon_2 \quad (A.9)$$

$$\delta^{13}C_{C_2H_6} = \delta^{13}C_a + \epsilon_1 + \epsilon_3 \quad (A.10)$$

$$\begin{aligned} \Delta^{13}C &= \delta^{13}C_{C_3H_8,pyrolyzed} - \delta^{13}C_{C_3H_8,original} \\ &= (X_{CH_4} + X_{C_2H_6}) \cdot \epsilon_1 + X_{C_2H_4} \cdot \epsilon_1/2 + X_{C_3H_6} \cdot \epsilon_2 \end{aligned} \quad (A.11)$$

The detailed procedure to calculate  $\epsilon$  values is as follows:

$$(A.10) - (A.7) \rightarrow \epsilon_3 = \delta^{13}C_{C_2H_6} - \delta^{13}C_{CH_4,corrected}, \quad (A.12)$$

$$\begin{aligned} (A.8) \times 2 + (A.7) - (A.9) \times 3 &\rightarrow 2\epsilon_1 - 3\epsilon_2 \\ &= C_{CH_4,corrected} + 2\delta^{13}C_{C_2H_4} - 3\delta^{13}C_{C_3H_6}, \end{aligned} \quad (A.13)$$

Combining Eqs. (A.11) and (A.13) gives values for  $\epsilon_1$  and  $\epsilon_2$  as follows:

$$\epsilon_1 = \frac{\Delta^{13}C + X_{C_3H_6} \times \left( \frac{1}{3}\delta^{13}C_{CH_4,corrected} + \frac{2}{3}\delta^{13}C_{C_2H_4} - \delta^{13}C_{C_3H_6} \right)}{X_{CH_4} + \frac{1}{2}X_{C_2H_4} + X_{C_2H_6} + \frac{2}{3}X_{C_3H_6}} \quad (A.14)$$

and

$$\epsilon_2 = \frac{\Delta^{13}C - (X_{CH_4} + \frac{1}{2}X_{C_2H_4} + X_{C_2H_6}) \times \left( \frac{1}{2}\delta^{13}C_{CH_4,corrected} + \delta^{13}C_{C_2H_4} - \frac{3}{2}\delta^{13}C_{C_3H_6} \right)}{\frac{3}{2}X_{CH_4} + \frac{3}{4}X_{C_2H_4} + \frac{3}{2}X_{C_2H_6} + X_{C_3H_6}} \quad (A.15)$$

The value of  $\delta^{13}C_{CH_4,corrected}$  can be calculated as follows:

$$\delta^{13}C_{CH_4,corrected} = (m_{CH_4} \times \delta^{13}C_{CH_4} + 2m_{C_2H_6} \times \delta^{13}C_{C_2H_6}) / (m_{CH_4} + 2m_{C_2H_6}) \quad (A.16)$$

where  $m_{CH_4}$  and  $m_{C_2H_6}$  are the molar yields of pyrolysis fragments  $CH_4$  and  $C_2H_6$ , respectively, and  $\delta^{13}C_{CH_4}$  and  $\delta^{13}C_{C_2H_6}$  are the carbon isotope compositions of  $CH_4$  and  $C_2H_6$ , respectively. The molar yields of the pyrolysis fragments can be obtained according to the quantification of pyrolysis products (data in Fig. 3).

The value of  $\delta^{13}C_{C_3H_8,pyrolyzed}$  can be obtained from Eqs. (A.17) and (A.18):

$$\begin{aligned} \delta^{13}C_{C_3H_8,pyrolyzed} &= (X_{CH_4} \cdot \delta^{13}C_{CH_4} + X_{C_2H_4} \cdot \delta^{13}C_{C_2H_4} + X_{C_2H_6} \\ &\quad \cdot \delta^{13}C_{C_2H_6} + X_{C_3H_6} \cdot \delta^{13}C_{C_3H_6}) \end{aligned} \quad (A.17)$$

$$X_i = \frac{m_i \cdot n_i}{\sum m_i \cdot n_i} = \frac{m_i \cdot n_i}{m_{CH_4} + m_{C_2H_4} \cdot 2 + m_{C_2H_6} \cdot 2 + m_{C_3H_6} \cdot 3}, \quad (A.18)$$

where  $i$  represents fragments  $CH_4$ ,  $C_2H_4$ ,  $C_2H_6$ , and  $C_3H_6$ , and  $X_i$  is the mass fraction of carbon content for fragment  $i$  in the pyrolytic products,  $n_i$  is the number of carbon atoms in fragment  $i$ , and  $m_i$  is the molar yield of pyrolytic fragment  $i$ , which can be obtained according to the quantification of pyrolysis products (data in Fig. 3).

When the values of  $\delta^{13}C_{CH_4,corrected}$  and  $\Delta^{13}C$  have been obtained based on Eqs. (A.16) and (A.11), respectively, and values of  $X_{CH_4}$ ,  $X_{C_2H_4}$ ,  $X_{C_2H_6}$ , and  $X_{C_3H_6}$  have been obtained following Eq. (A.18),  $\epsilon$  values can be calculated according to Eqs. (A.12), (A.14), and (A.15).

Associate Editor—Joe Curiale

## References

- Abelson, P.H., Hoering, T.C., 1961. Carbon isotope fractionation in formation of amino acids by photosynthetic organisms. *Proceedings of the National Academy of Sciences of the United States of America* 47, 623–632.
- Caer, V., Trierweiler, M., Martin, G.J., Martin, M.L., 1991. Determination of site-specific carbon isotope ratios at natural abundance by carbon-13 nuclear magnetic resonance spectroscopy. *Analytical Chemistry* 63, 2306–2313.
- Caytan, E., Botosoa, E.P., Silvestre, V., Robins, R.J., Akoka, S., Remaud, G.S., 2007. Accurate quantitative  $^{13}C$  NMR spectroscopy: repeatability over time of site-specific  $^{13}C$  isotope ratio determination. *Analytical Chemistry* 79, 8266–8269.
- Corso, T.N., Brenna, J.T., 1997. High-precision position-specific isotope analysis. *Proceedings of the National Academy of Sciences of the United States of America* 94, 1049–1053.
- Corso, T.N., Brenna, J.T., 1999. On-line pyrolysis of hydrocarbons coupled to high-precision carbon isotope ratio analysis. *Analytica Chimica Acta* 397, 217–224.
- Corso, T.N., Lewis, B., Brenna, J.T., 1998. Reduction of fatty acid methyl esters to fatty alcohols to improve volatility for isotopic analysis without extraneous carbon. *Analytical Chemistry* 70, 3752–3756.
- Dias, R.F., Freeman, K.H., Franks, S.G., 2002. Gas chromatography–pyrolysis–isotope ratio mass spectrometry: a new method for investigating intramolecular isotopic variation in low molecular weight organic acids. *Organic Geochemistry* 33, 161–168.
- Eiler, J.M., Clog, M., Magyar, P., Piasecki, A., Sessions, A., Stolper, D., Deerberg, M., Schlueter, H.J., Schwieters, J., 2013. A high-resolution gas-source isotope ratio mass spectrometer. *International Journal of Mass Spectrometry* 335, 45–56.
- Galimov, E.M., 1988. Sources and mechanisms of formation of gaseous hydrocarbons in sedimentary rocks. *Chemical Geology* 71, 77–95.
- Gao, L., He, P.Q., Jin, Y.B., Zhang, Y.Q., Wang, X.Q., Zhang, S.C., Tang, Y.C., 2016. Determination of position-specific carbon isotope ratios in propane from hydrocarbon gas mixtures. *Chemical Geology* 435, 1–9.
- Gauchotte, C., O'Sullivan, G., Davis, S., Kalin, R.M., 2009. Development of an advanced on-line position-specific stable carbon isotope system and application to methyl tert-butyl ether. *Rapid Communications in Mass Spectrometry* 23, 3183–3193.
- Gauchotte-Lindsay, C., Turnbull, S.M., 2016. On-line high-precision carbon position-specific stable isotope analysis: a review. *Trac-Trends in Analytical Chemistry* 76, 115–125.
- Gilbert, A., Yamada, K., Suda, K., Ueno, Y., Yoshida, N., 2016. Measurement of position-specific  $^{13}C$  isotopic composition of propane at the nanomole level. *Geochimica et Cosmochimica Acta* 177, 205–216.
- Hattori, R., Yamada, K., Kikuchi, M., Hirano, S., Yoshida, N., 2011. Intramolecular carbon isotope distribution of acetic acid in vinegar. *Journal of Agricultural and Food Chemistry* 59, 9049–9053.
- Hayes, J.M., Freeman, K.H., Popp, B.N., Hoham, C.H., 1990. Compound-specific isotopic analyses: a novel tool for reconstruction of ancient biogeochemical processes. *Organic Geochemistry* 16, 1115–1128.
- James, A.T., 1983. Correlation of natural gas by use of carbon isotopic distribution between hydrocarbon components. *Bulletin of the American Association of Petroleum Geologists* 67, 1167–1191.
- James, A.T., 1990. Correlation of reservoir gases using the carbon isotopic compositions of wet gas components. *Bulletin of the American Association of Petroleum Geologists* 74, 1441–1458.
- Julien, M., Nun, P., Robins, R.J., Remaud, G.S., Parinet, J., Höhener, P., 2015. Insights into mechanistic models for evaporation of organic liquids in the environment obtained by position-specific carbon isotope analysis. *Environmental Science & Technology* 49, 12782–12788.
- Layokun, S.K., Slater, D.H., 1979. Mechanism and kinetics of propane pyrolysis. *Industrial Engineering Chemistry Research* 18, 232–236.
- Monson, D.K., Hayes, J.M., 1982. Carbon isotope fractionation in the saturated fatty acids as a mean of determining the intramolecular distribution of carbon isotopes. *Geochimica et Cosmochimica Acta* 46, 139–149.
- Piasecki, A., Sessions, A., Lawson, M., Ferreira, A.A., Neto, E.V.S., Eiler, J.M., 2016. Analysis of the site-specific carbon isotope composition of propane by gas source isotope ratio mass spectrometer. *Geochimica et Cosmochimica Acta* 188, 58–72.
- Piasecki, A., Sessions, A., Lawson, M., Ferreira, A.A., Neto, E.V.S., Ellis, G.S., Lewan, M. D.L., Eiler, J.M., 2018. Position-specific  $^{13}C$  distributions within propane from experiments and natural gas samples. *Geochimica et Cosmochimica Acta* 220, 110–124.
- Rooney, M.A., Claypool, G.E., Chung, H.M., 1995. Modeling thermogenic gas generation using carbon isotope ratios of natural gas hydrocarbons. *Chemical Geology* 126, 219–232.
- Sacks, G.L., Brenna, J.T., 2003. High-precision position-specific isotope analysis of  $^{13}C/^{12}C$  in leucine and methionine analogues. *Analytical Chemistry* 75, 5495–5503.

- Schoell, M., 1983. Genetic characterization of natural gases. *Bulletin of the American Association of Petroleum Geologists* 67, 2225–2238.
- Schoell, M., 1988. Multiple origins of methane in the Earth. *Chemical Geology* 71, 1–10.
- Suda, K., Gilbert, A., Yamada, K., Yoshida, N., Ueno, Y., 2017. Compound- and position-specific carbon isotopic signatures of abiogenic hydrocarbons from on-land serpentinite-hosted Hakuba Happo hot spring in Japan. *Geochimica et Cosmochimica Acta* 206, 201–215.
- Tuli, J.K., 1985. Nuclear Wallet Cards. Natural Nuclear Data Center, Brookhaven National Laboratory, p. 35.
- Wang, Z.G., Schauble, E.A., Eiler, J.M., 2004. Equilibrium thermodynamics of multiply substituted isotopologues of molecular gases. *Geochimica et Cosmochimica Acta* 68, 4779–4797.
- Wolyniak, C.J., Sacks, G.L., Pan, B.S., Brenna, J.T., 2005. Carbon position-specific isotope analysis of alanine and phenylalanine analogues exhibiting nonideal pyrolytic fragmentation. *Analytical Chemistry* 77, 1746–1752.
- Wolyniak, C.J., Sacks, G.L., Metzger, S.K., Brenna, J.T., 2006. Determination of intramolecular  $\delta^{13}\text{C}$  from incomplete pyrolysis fragments. Evaluation of pyrolysis-induced isotopic fractionation in fragments from the lactic acid analogue propylene glycol. *Analytical Chemistry* 78, 2752–2757.
- Yamada, K., Tanaka, M., Nakagawa, F., Yoshida, N., 2002. On-line measurement of intramolecular carbon isotope distribution of acetic acid by continuous-flow isotope ratio mass spectrometry. *Rapid Communication in Mass Spectrometry* 16, 1059–1064.
- Zhang, B.L., Buddrus, S., Trierweiler, M., Martin, G.J., 1998. Characterization of glycerol from different origins by  $^2\text{H}$ - and  $^{13}\text{C}$ -NMR studies of site-specific natural isotope fractionation. *Journal of Agricultural and Food Chemistry* 46, 1374–1380.
- Zhang, B.L., Trierweiler, M., Joutteau, C., Martin, G.J., 1999. Consistency of NMR and mass spectrometry determinations of natural abundance site-specific carbon isotope ratios. The case of glycerol. *Analytical Chemistry* 71, 2301–2306.